# Hepatic organic anion transporting polypeptides mediate disposition of milk thistle flavonolignans and pharmacokinetic silymarin-drug interactions

By: Katherine D. Lynch, Michelle L. Montonye, Dan-Dan Tian, Tarana Arman, Victoria O. Oyanna, Baron J. Bechtold, Tyler N. Graf, Nicholas H. Oberlies, Mary F. Paine, and John D. Clarke

**This is the peer reviewed version of the following article:**

Katherine D. Lynch, Michelle L. Montonye, Dan-Dan Tian, Tarana Arman, Victoria O. Oyanna, Baron J. Bechtold, Tyler N. Graf, Nicholas H. Oberlies, Mary F. Paine, and John D. Clarke. Hepatic organic anion transporting polypeptides mediate disposition of milk thistle flavonolignans and pharmacokinetic silymarin-drug interactions. *Phytotherapy Research*. 2021; 1– 12. https://doi.org/10.1002/ptr.7049

**which has been published in final form at https://doi.org/10.1002/ptr.7049. This article may be used for non-commercial purposes in accordance with Wiley Terms and Conditions for Use of Self-Archived Versions.**



## Abstract:

*Silybum marianum* (L.) Gaertn. (Asteraceae), commonly known as milk thistle, is a botanical natural product used to self-treat multiple diseases such as Type 2 diabetes mellitus and nonalcoholic steatohepatitis (NASH). An extract from milk thistle seeds (achenes), termed silymarin, is comprised primarily of several flavonolignans. Systemic concentrations of these flavonolignans can influence the potential biologic effects of silymarin and the risk for pharmacokinetic silymarin-drug interactions. The aims of this research were to determine the roles of organic anion transporting polypeptides (OATPs/Oatps) in silymarin flavonolignan disposition and in pharmacokinetic silymarin-drug interactions. The seven major flavonolignans from silymarin were determined to be substrates for OATP1B1, OATP1B3, and OATP2B1. Sprague Dawley rats were fed either a control diet or a NASH-inducing diet and administered pitavastatin (OATP/Oatp probe substrate), followed by silymarin via oral gavage. Decreased protein expression of Oatp1b2 and Oatp1a4 in NASH animals increased flavonolignan area under the plasma concentration-time curve (AUC) and maximum plasma concentration. The combination of silymarin inhibition of Oatps and NASH-associated decrease in Oatp expression caused an additive increase in plasma pitavastatin AUC in the animals. These data indicate that OATPs/Oatps contribute to flavonolignan cellular uptake and mediate the interaction between silymarin and NASH on pitavastatin systemic exposure.

**Keywords:** flavonolignans | nonalcoholic steatohepatitis | organic anion transporting polypeptide | pharmacokinetics | pitavastatin | silymarin

**Article:**

## 1 INTRODUCTION

*Silybum marianum* (L.) Gaertn. (Asteraceae), commonly known as milk thistle, was ranked 10th and 23rd in U.S. natural channel and U.S. mainstream multi-outlet sales, respectively, amassing more than $26 million in sales in 2019 (Smith, May, Eckl, & Reynolds, 2020). An extract of milk thistle seeds, termed silymarin, consists of ~50–70% flavonolignans (e.g., silybin A [SA], silybin B [SB], isosilybin A [IA], isosilybin B [IB], silydianin [SD], silychristin [SC]) and flavonoids (e.g., taxifolin, quercetin), with the remaining ~30–50% consisting of chemically undefined polyphenolic compounds (Graf, Cech, Polyak, & Oberlies, 2016; Javed, Kohli, & Ali, 2011). Various forms of milk thistle have been used for centuries to treat multiple disorders, including liver diseases and mushroom poisoning (Abenavoli et al., 2018; Smith et al., 2020). More recently, silymarin has been investigated as a therapeutic agent for multiple diseases, including viral hepatitis, Type 2 diabetes mellitus, alcoholic liver disease, cholestasis, drug- or toxin-induced liver disease, primary liver malignancies, nonalcoholic fatty liver disease (NAFLD), and nonalcoholic steatohepatitis (NASH) (Abenavoli et al., 2018; Voroneanu, Nistor, Dumea, Apetrii, & Covic, 2016). Silymarin is also marketed to the "healthy" population as a liver detoxification product, as well as to offset the effects of alcohol consumption (Feher & Lengyel, 2012; Lieber, Leo, Cao, Ren, & DeCarli, 2003; Müzes et al., 1990).

Efficacy of silymarin as a treatment for various liver diseases is equivocal, but the doses and formulations that produce micromolar flavonolignan systemic plasma concentrations are well tolerated in healthy and liver diseased populations (Fried et al., 2012; Wah Kheong, Nik Mustapha, & Mahadeva, 2017). For example, up to 2.1 g per day of silymarin administered to NASH patients caused no adverse events (Wah Kheong et al., 2017). Similarly, 13 g per day of a phytosome formulation consisting of silybin A, silybin B, and phosphatidylcholine produced flavonolignan plasma concentrations up to 75 μM and caused no adverse events in prostate cancer patients (Flaig et al., 2007). Flavonolignan systemic concentrations are influenced by uptake transporters, metabolizing enzymes, and efflux transporters, and can influence the biologic effects and pharmacokinetic drug interaction liability of silymarin. Enteric absorption and hepatic clearance of flavonolignans are mediated by the efflux transporters multidrug resistance-associated protein (MRP)2, MRP3, MRP4, and breast cancer resistance protein (BCRP; Bi et al., 2019; Miranda et al., 2008; Schrieber et al., 2011; Wlcek, Koller, Ferenci, & Stieger, 2013; Xu et al., 2018). Organic anion transporting polypeptides (OATPs/Oatps) have been speculated as flavonolignan uptake transporters, although no direct mechanistic data have been collected.

OATPs/Oatps belong to a superfamily of transporters that mediate the sodium-independent transport of a wide range of amphiphilic organic compounds, including many hydroxymethylglutaryl-CoA reductase inhibitors (statins), angiotensin II receptor blockers, angiotensin converting enzyme inhibitors, chemotherapeutic agents, and antidiabetic agents (Giacomini et al., 2010; Maeda, 2015). Common notation to distinguish human versus rodent OATP/Oatp isoforms is uppercase versus lowercase, respectively (Hagenbuch & Meier, 2004). The rate-limiting step in the hepatic clearance of OATP/Oatp substrates can be uptake from portal blood into the liver (Maeda, 2015), and silymarin has been investigated as a potential

precipitant of natural product-drug interactions involving OATPs/Oatps (Deng et al., 2008). Intravenous administration of silymarin to Sprague Dawley rats was recently shown to inhibit Oatp-mediated pitavastatin uptake and increase the area under the plasma concentration-time curve (AUC) of intravenously administered pitavastatin, a probe for OATPs/Oatps (Montonye et al., 2019). Although these data provided fundamental pharmacokinetic information, both silymarin and pitavastatin are taken orally by patients with healthy livers and NASH patients, and risk for a pharmacokinetic interaction after oral consumption is unknown.

The purpose of the present study was to evaluate a probable natural product-disease-drug interaction in a preclinical model. The were two aims in this study. The first was to determine the role of OATPs/Oatps in flavonolignan disposition. The information gained can be used to predict populations with altered flavonolignan disposition or to exploit these mechanisms to alter flavonolignan disposition and augment potential beneficial effects. The second was to determine whether oral silymarin administration can precipitate pharmacokinetic drug interactions involving Oatps in healthy versus NASH animals. By using a NASH rodent model that recapitulates important clinical features related to drug disposition (Canet et al., 2014), information from this research can justify and inform investigation of this natural product-disease-drug interaction in humans.

## 2 MATERIALS AND METHODS

### 2.1 Chemicals and reagents

Pitavastatin calcium (cat.# ab141958, >98% purity) was purchased from Abcam (Cambridge, MA). Pitavastatin-$d_5$ (cat.# P531022) was purchased from Toronto Research Chemicals (Ontario, Canada). Naringin (cat.# 71162-25G, >95% purity), dichlorofluorescein (cat.# 35848-5G, >90% purity), dibromofluorescein (cat.# 216,720-5 g, >95% purity), and silymarin (cat.# S0292, lot no. BCBT9170) were purchased from Sigma Aldrich (St. Louis, MO). The silymarin lot was characterized previously (Montonye et al., 2019). Fluorescein (cat.# 97062–186) and sodium butyrate (cat.# AAA11079-36, >98% purity) were purchased from VWR (Radnor, PA). Geneticin (cat.# 10-131-027) was purchased from Thermo Fisher Scientific (Waltham, MA). Flavonolignans were isolated from silymarin using a hybrid chromatographic/precipitative technique as detailed previously (Graf, Wani, Agarwal, Kroll, & Oberlies, 2007). Reference standards for glucuronides of the silymarin flavonolignans were generated using bovine liver microsomes as detailed previously (Gufford, Graf, Paguigan, Oberlies, & Paine, 2015). All flavonolignan reference standards were validated to be greater than 95% pure, as measured by UPLC (Graf et al., 2016). Control diet (cat.# TD180070) and standard diet (cat.# 2016) were purchased from Envigo (Madison, WI). The methionine-and choline-deficient (MCD) diet (cat.# D518810) was purchased from Dyets Inc. (Bethlehem, PA). Wild-type Chinese hamster ovary (CHO) cells and CHO cells stably expressing human OATP1B1, OATP1B3, or OATP2B1 were provided by Dr. Bruno Stieger (University of Zurich, Zurich, Switzerland). Antibodies used in western blots were as follows: Oatp1b2 (cat.# 376904, Santa Cruz Biotechnology, Santa Cruz, CA) visualized with an antimouse HRP-labeled secondary antibody; and Oatp1a4 (cat.# OATP21-A, Alpha diagnostics, San Antonio, TX) visualized with an anti-rabbit HRP-labeled secondary antibody. SuperSignal West Pico and Femto (ThermoFisher Scientific) were used as chemiluminescent substrates to visualize proteins of interest. Guidelines relevant to best

practices in natural products research were considered throughout the study (Heinrich et al., 2020; Izzo et al., 2020; Kellogg, Paine, McCune, Oberlies, & Cech, 2019).

## 2.2 Animals

Handling, care, and maintenance of the animals took place in the Program of the Laboratory Animal Resources facility of Washington State University Health Sciences Spokane, which is accredited by the Association for the Assessment of Laboratory Animal Care International. The experimental protocol was approved by the Institutional Animal Care and Use Committee at Washington State University. Eight-week-old male Sprague Dawley rats ($n = 26$) were purchased from Envigo (Huntingdon, Cambridgeshire, UK). Animals were randomly placed in cages (two per cage) with diamond soft-paper bedding and fed a control diet for 16 weeks ($n = 14$) or standard diet for 8 weeks followed by an MCD diet for 8 weeks ($n = 12$). Silymarin and pitavastatin were prepared as previously described (Montonye et al., 2019). Silymarin vehicle consisted of 20% propylene glycol, 45% PEG400, and 35% molecular grade water. After the diet period, animals were fasted for 12 hr, then pitavastatin (2.5 mg/kg, 5 ml/kg), dissolved in DMSO, and diluted in sterile saline (2% DMSO final), was administered by oral gavage. Forty minutes after administration of pitavastatin, vehicle (10 ml/kg) or silymarin (500 mg/kg, 10 ml/kg) was administered by oral gavage. The dose of silymarin was selected to produce flavonolignan plasma concentrations observed in humans. Published clinical pharmacokinetic studies involving NAFLD and HCV patients reported average $C_{max}$ values for silybin A between 0.8 and 4.2 μM (Fried, 2012; Wah Kheong et al., 2017). This dose of silymarin was also shown to be safe in rodents (Gao et al., 2018). Blood (~0.2 ml) was collected through the tail vein into heparinized tubes at 0.083, 0.25, 0.5, 0.75, 0.83, 1, 1.5, 2, 4, 6, 9, and 12 hr after the first gavage. Animals were euthanized 27 hr after the first gavage. Plasma was isolated by centrifugation, and interconversion between the acid and lactone forms of pitavastatin was prevented by acidifying plasma samples as previously described (Montonye et al., 2019; Qi et al., 2013). After the terminal blood was collected, animals were euthanized by carbon dioxide asphyxiation and exsanguination, and livers were harvested as previously described (Montonye et al., 2019). Liver samples were formalin fixed and paraffin embedded or snap frozen in liquid nitrogen and stored at −80°C until further analyses.

## 2.3 Cell culture

Wild-type CHO cells and CHO cells stably expressing human OATP1B1 (passages 28–37), OATP1B3 (passages 27–36), or OATP2B1 (passages 20–29) were maintained at 37°C in a humidified 5% $CO_2$ atmosphere in Dulbecco's modified Eagle's medium (low-glucose) containing 25 mM HEPES, supplemented with 10% fetal bovine serum, and 50 mg/ml L-proline culture without geneticin for wild-type cells and with 0.5 mg/ml geneticin for OATP-expressing cells. Cells were seeded onto 12-well plates at a density of $0.3 \times 10^6$ cells per well. Transporter expression was induced by incubating cells with 10 mM sodium butyrate for 24 hr prior to transport experiments. Waymouth transport buffer (135 mM sodium chloride, 1.3 mM HEPES, 2.8 mM D-glucose, 0.5 mM potassium chloride, 0.25 mM calcium dichloride, 0.12 mM magnesium dichloride, 80 mM magnesium sulfate, pH 7.4) was used in place of culture medium for all transport experiments. Prior to initiating transport, cells were washed three times with prewarmed transport buffer and allowed to equilibrate for 5 min at 37°C. Transport was

normalized to total cellular protein as quantified by the Pierce BCA assay (Thermo Fisher Scientific) using a Synergy H1 (BioTek, Winooski, VT) plate reader.

*2.3.1 $IC_{50}$ determination*

Uptake was initiated by addition of prewarmed transport buffer containing 5 μM dichlorofluorescein (OATP1B1 probe), 5 μM fluorescein (OATP1B3 probe), or 2 μM dibromofluorescein (OATP2B1 probe), with increasing silymarin concentrations (0–48 μg/ml). No change in cell viability was observed at these concentrations for this short incubation period (data not shown). For preincubation experiments, each cell line was incubated with transport buffer containing silymarin for 35 min at 37°C before addition of transport buffer containing fluorescent probe substrate. Transport was terminated at 5 min for OATP1B1 and OATP1B3, or 2 min for OATP2B1, with ice-cold transport buffer. Cells were washed quickly three times with ice-cold transport buffer before being lysed with 110 μl of milliQ water. Plates were subjected to a freeze-thaw cycle at −80°C before the wells were scraped and samples transferred to microcentrifuge tubes. Supernatant (80 μl) was analyzed using a fluorescence microplate reader (Synergy H1) at the following excitation/emission wavelengths: dichlorofluorescein, 460 nm/515 nm; dibromofluorescein, 485 nm/528 nm; and fluorescein, 460 nm/515 nm. Autofluorescence of cells without substrate was subtracted from the fluorescence measured in cells incubated with substrate before comparing to the calibration curve. Quantification of unknowns was accomplished using a calibration curve that was linear from 1.0 to 500 nM for each fluorescent compound. Dichlorofluorescein, fluorescein, and dibromofluorescein substrate choices were based on a previously published method (Izumi et al., 2016). Substrate concentrations and incubation times were validated prior to experimentation (data not shown). Best-fit $IC_{50}$ values were determined by nonlinear least-squares regression using the standard Hill equation as previously described (Gufford et al., 2014) for all OATPs using GraphPad Prism (version 7.0; San Diego, CA).

*2.3.2 Flavonolignans as substrates*

Uptake was initiated by addition of prewarmed transport buffer containing 5 μM of flavonolignan; transport was terminated at 5 min with ice-cold transport buffer. Cells were washed quickly three times with ice-cold transport buffer before being lysed with 110 μl of 0.1% formic acid in HPLC water. Plates were subjected to a freeze–thaw cycle at −80°C before the wells were scraped, after which cell lysates were transferred to microcentrifuge tubes. Cell lysate (80 μl) was mixed with 320 μl of 0.028 μM naringin (internal standard) in acetonitrile; proteins were precipitated by centrifugation at 13,000*g* for 5 min at room temperature. The supernatant (380 μl) was dried under vacuum at 37°C, then reconstituted in 50 μl of 20% methanol with 0.1% formic acid and analyzed for flavonolignans as described below via liquid chromatography/mass spectrometry. OATP-mediated transport was calculated by subtracting intracellular substrate concentrations in wild-type CHO cells from intracellular substrate concentrations in OATP-expressing CHO cells.

2.4 Liquid chromatography-mass spectrometry for pitavastatin

Quantification of pitavastatin was performed as previously described (Montonye et al., 2019). Briefly, 10 µl of plasma was mixed with 0.1% formic acid water containing internal standards followed by protein precipitation. Chromatographic separation and quantification were performed using a QTRAP 6500 UHPLC-MS/MS (AB Sciex, Framingham, MA) system. A gradient of 0.1% formic acid in water (A) and 0.1% formic acid in acetonitrile (B) was passed through an HSS T3 column (1.8 mm, 2.1 × 50 mm, Waters Corporation, Waltham, MA) at 50°C. The turbo electrospray source was operated in positive ionization mode. The following multiple reaction monitoring transitions were used for compound quantification: pitavastatin, 422.1 → 290.1 m/z; pitavastatin-$d_5$, 426.9 → 293.8 m/z. A second precursor-fragment ion combination was used to validate the presence of each compound. Plasma and liver samples were spiked with the internal standard, pitavastatin-$d_5$ (0.24 µM). Powdered 50 mg liver tissue was homogenized in 100 µl of 0.1% formic acid water containing 1.2 µM pitavastatin-$d_5$ and 6.2 µM pitavastatin lactone-$d_5$ internal standard. Liver pitavastatin content was calculated based on total liver weight. Liver to plasma ratio was calculated by dividing total liver pitavastatin content by the final concentration of pitavastatin in the plasma at 27 hr. Quantification of pitavastatin was accomplished using a calibration curve that was linear from 0.018 to 4.75 µM, and quality control samples (0.5 µM) were run periodically to ensure consistent instrument performance.

2.5 Liquid chromatography-mass spectrometry for flavonolignans

Quantification of flavonolignans from silymarin was performed as previously described (Montonye et al., 2019). Briefly, 20 µl of plasma were mixed with internal standard and 0.1% formic acid in methanol. See Section 2.3.2 for sample preparation methods after transport experiments. Chromatographic separation and quantification was performed on a QTRAP 6500. A gradient of 0.1% formic acid in water (A) and 0.1% formic acid in methanol (B) was passed through an HSS T3 column at 50°C. The turbo electrospray source was operated in the negative ionization mode. The following multiple reaction monitoring transitions were used for compound quantification: silybin A, 480.9 → 301.9 m/z; silybin B, 480.9 → 125.0 m/z; silychristin, 480.9 → 325.1 m/z; silydianin, 480.9 → 178.9 m/z; isosilybin A, 480.9 → 125.0 m/z; isosilybin B, 480.9 → 125.0 m/z; isosilychristin, 480.9 → 463.0; taxifolin, 302.8 → 284.9 m/z; silybin A and silybin B glucuronides, 657.1 → 481.1; naringin, 578.9 → 270.9. A second precursor-product ion pair was used to validate the presence of each compound. Plasma samples were spiked with naringin as internal standard (0.17 µM). Flavonolignans in cell culture experiments were quantified as described above. Quantification of flavonolignans was accomplished using a calibration curve that was linear from 0.016 to 4.16 µM, and quality control samples (0.06 and 0.13 µM) were run periodically to ensure consistent instrument performance.

2.6 Western blot analysis

Liver protein samples were extracted as previously described (Montonye et al., 2019). Briefly, liver tissue was homogenized in NP-40 lysis buffer using a TissueLyzer II (Qiagen, Hilden, Germany). Total protein (20 µg) was prepared in Laemmli sample buffer containing 2.5% 2-mercaptoethanol and heated at 37°C for 30 min. Samples were loaded onto 7.5% SDS-PAGE gels and transferred to polyvinylidene difluoride membranes using a Bio-Rad (Hercules, CA) Trans-Blot Turbo system at 25 V/1.0 A for 30 min. Membranes were blocked with 5% nonfat dry milk in Tris-buffered saline/Tween 20 and incubated with the following antibodies: Oatp1b2

1:1,000; mouse secondary 1:10,000; Oatp1a4 1:1,000; rabbit secondary 1:10,000. Signal was developed with SuperSignal West Pico for Oatp1b2 and Femto for Oatp1a4. Densitometry was performed using Image Lab (Bio-Rad, Standard Edition, Version 6.0.0 build 25). Proteins of interest were normalized to total protein as determined by Amido black staining (Aldridge, Podrebarac, Greenough, & Weiler, 2008).

### 2.7 Pharmacokinetic analysis

The pharmacokinetics of flavonolignans, taxifolin, and pitavastatin were determined via non-compartmental analysis methods using Phoenix (version 7.0; Certara, Princeton, NJ). $C_{max}$ and time to reach $C_{max}$ ($t_{max}$) were obtained directly from the concentration-time profile. Partial AUC was determined using the linear up/log down trapezoidal method (0–27 hr for flavonolignan glucuronides and pitavastatin and 0–2 hr for SC and TF). When appropriate (i.e., sufficient data points were available), terminal slope ($\lambda_z$) was recovered via linear regression of at least the last four data points, and terminal half-life ($t_{1/2}$) was calculated as the ratio of 0.693 to $\lambda_z$. Total AUC ($AUC_{inf}$) for SA, SB, IA, and IB was calculated as the sum of $AUC_{0\text{-}27h}$ and the ratio of the last measured concentration to $\lambda_z$. Oral clearance (Cl/F) was calculated as the ratio of dose to $AUC_{inf}$.

### 2.8 Statistical analysis

Two-way analysis of variance (ANOVA) *p*-values are shown in tables accompanying the respective graph and in Table 2. Bonferroni post hoc test was used when comparing pitavastatin pharmacokinetic and protein expression data among the control and NASH groups, with or without silymarin. Flavonolignan comparisons between control and NASH groups were made using the unpaired Student's *t* test. AUC, $C_{max}$, and Cl/F values were log-transformed prior to statistical analysis. $T_{max}$ values were analyzed with the Mann–Whitney *U* test. No randomization or blinding was performed for these analyses.

## 3 RESULTS AND DISCUSSION

### 3.1 Role of OATPs/Oatps in silymarin disposition

Silymarin exposure time and concentration are important considerations for understanding potential beneficial or detrimental biologic effects. In the current study, average unconjugated flavonolignan plasma AUC and $C_{max}$ values after oral administration of silymarin (Figure 1 and Table 1) were congruent with relative proportions observed in healthy human volunteers (SA = SB=IA = IB> > SC=SD) (Wen et al., 2008). AUC and $C_{max}$ for individual flavonolignans and taxifolin were 2.2- to 2.5-fold and 2.4- to 3.5-fold higher, respectively, whereas corresponding Cl/F was 53–72% lower, in the NASH group compared to the control group (Table 1). These data are consistent with a previous clinical study in hepatitis C virus (HCV) and NAFLD patients in which total plasma flavonolignan AUC was 2.4- and 3.3-fold higher, respectively, than in healthy volunteers (Schrieber et al., 2011). $AUC_{0\text{-}27h}$ and $C_{max}$ for SA and SB glucuronides in the current study were 3.6-fold and 4.2- to 6.3-fold higher, respectively, in the NASH group compared to the control group (Table 1). These data show increased plasma concentrations of both the unconjugated flavonolignans and glucuronides in NASH, suggesting a mechanism

involving enteric and/or hepatic transporters rather than phase II metabolism (Schrieber et al., 2008, 2011).

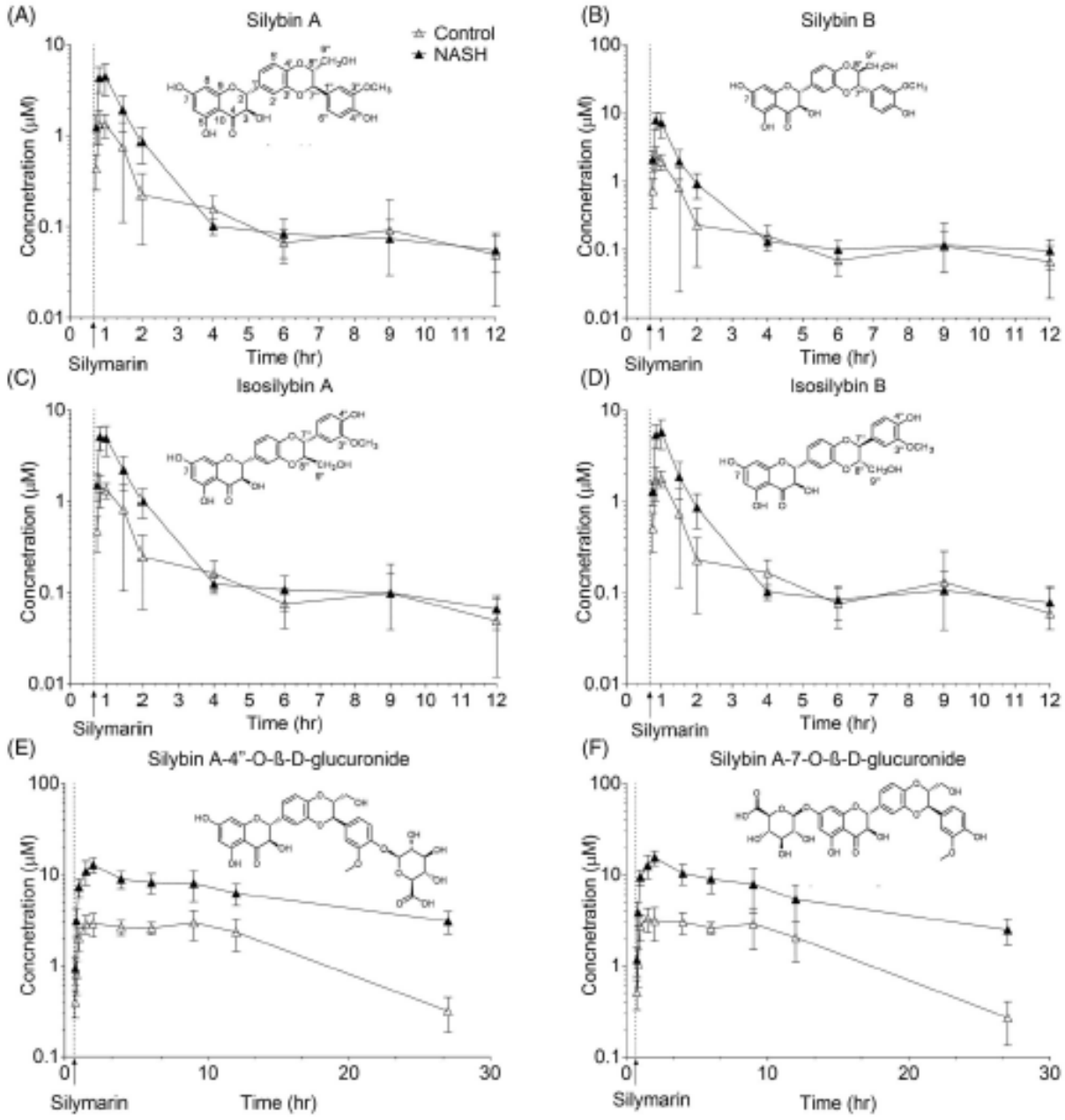


**FIGURE 1.** Silymarin flavonolignan plasma concentration versus time profiles and structures. Plasma exposure to silymarin flavonolignans and glucuronides is higher in NASH compared to control animals. Average plasma concentration versus time profiles and chemical structures for silybin A (a), silybin B (b), isosilybin A (c), isosilybin B (d), silybin A-4″-O-β-d-glucuronide (e), and silybin A-7-O-β-d-glucuronide (f) following oral gavage of silymarin (500 mg/kg) to control and NASH animals. Symbols and error bars represent means and *SD*s, respectively, of control ($n = 7$) and NASH ($n = 6$) animals

**TABLE 1.** Silymarin flavonolignan and taxifolin plasma pharmacokinetics

| | | AUC (h*µmol/L) | Cl/F (L/h/kg) | $C_{max}$ (µmol/L) | $t_{1/2}$ (h) | $t_{max}$ (h) |
|---|---|---|---|---|---|---|
| SA | Control | 2.3 (1.8, 2.9) | 37.8 (29.9, 47.6) | 1.6 (1.3, 2.0) | 3.3 (2.7, 3.9) | 0.8 (0.83, 1.5) |
| | NASH | 4.9 (3.8, 6.5)* | 17.6 (13.4, 23.2)* | 4.5 (3.4, 6.0)* | 2.9 (2.0, 4.2) | 1.0 (0.83, 1.0) |
| SB | Control | 3.1 (2.3, 4.1) | 50.8 (37.7, 68.4) | 2.4 (1.9, 3.0) | 4.1 (2.7, 6.3) | 0.83 (0.83, 1.5) |
| | NASH | 10.9 (6.3, 18.9)* | 14.3 (8.2, 24.7)* | 7.9 (6.2, 10.2)* | 16.9 (2.9, 98.7) | 0.83 (0.83, 1.0) |
| IA | Control | 2.4 (1.9, 3.1) | 20.9 (16.5, 27.1) | 1.7 (1.4, 2.0) | 4.5 (2.9, 7.2) | 0.83 (0.83, 1.5) |
| | NASH | 7.5 (5.3, 10.6)* | 6.8 (4.8, 9.8)* | 5.2 (4.1, 6.7)* | 10.8 (0.6, 36.3) | 0.83 (0.83, 1.0) |
| IB | Control | 3.0 (2.2, 4.0) | 8.4 (6.2, 11.4) | 1.9 (1.6, 2.4) | 4.9 (3.0, 8.0) | 0.83 (0.83, 1.50) |
| | NASH | 7.9 (4.0, 15.6)* | 3.1 (1.6, 6.2)* | 5.9 (4.6, 7.5)* | 14.2 (3.9, 50.6) | 1.0 (0.83, 1.0) |
| SC | Control | 0.02 (0.01, 0.02) | NA | 0.02 (0.02, 0.03) | NA | 1.0 (1.0, 1.5) |
| | NASH | 0.05 (0.04, 0.06)* | NA | 0.07 (0.05, 0.08)* | NA | 1.0 (0.83, 1.0) |
| TF | Control | 0.18 (0.14, 0.24) | NA | 0.3 (0.2, 0.3) | NA | 0.83 (0.75, 1.5) |
| | NASH | 0.44 (0.30, 0.63)* | NA | 0.7 (0.5, 0.9)* | NA | 0.83 (0.83, 1.0) |
| S4G | Control | 44.5 (40.9, 48.4) | NA | 2.0 (2.5, 3.6) | NA | 2.0 (1.0, 2.0) |
| | NASH | 160.3 (141.2, 182.1)* | NA | 12.6 (10.6, 14.9)* | NA | 2.0 (2.0, 2.0) |
| S7G | Control | 43.0 (38.2, 48.5) | NA | 3.0 (2.5, 3.6) | NA | 2.0 (1.0, 2.0) |
| | NASH | 154.3 (129.1,184.5)* | NA | 12.6 (10.6,14.9)* | NA | 2.0 (2.0, 2.0) |

*Note:* Data represented as geometric means and upper and lower limits of 90% confidence intervals in parentheses for area under the plasma concentration time curve (AUC), oral clearance (Cl/F), maximum concentration ($C_{max}$), and half-life ($t_{1/2}$). Data for time to achieve $C_{max}$ ($t_{max}$) represent median with minimum and maximum in parentheses. NA = not applicable due to insufficient data points in the terminal phase of the plasma concentration-time profile. SB and IB are based on three animals in the NASH group, and IA is based on four animals in the NASH group. All other data shown are based on seven animals for control groups and six animals for NASH groups. Unpaired Student's *t* test.

Abbreviations: IA, isosilybin A; IB, isosilybin B; S4G, silybin A-4″-O-β-d-glucuronide; S7G, silybin A-7-O-β-d-glucuronide; SA, silybin A; SB, silybin B; SC, silychristin; TF, taxifolin. *p*-Values ≤.05 versus control silymarin group.

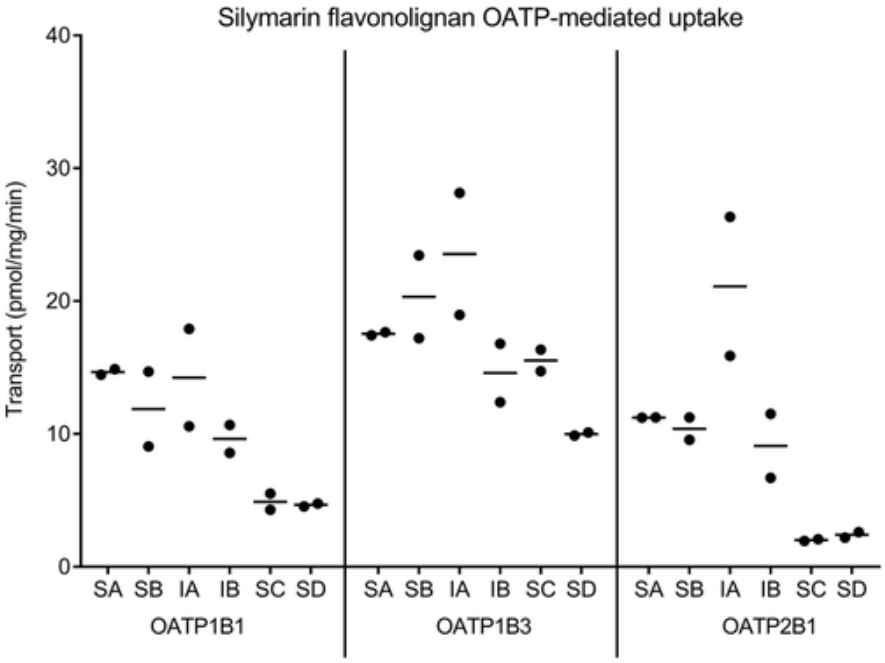


**FIGURE 2.** Silymarin flavonolignans are OATP substrates. Average OATP-mediated uptake of SA, SB, IA, IB, SC, and SD in OATP1B1, OATP1B3 and OATP2B1 expressing cells. Horizontal lines represent means of duplicates

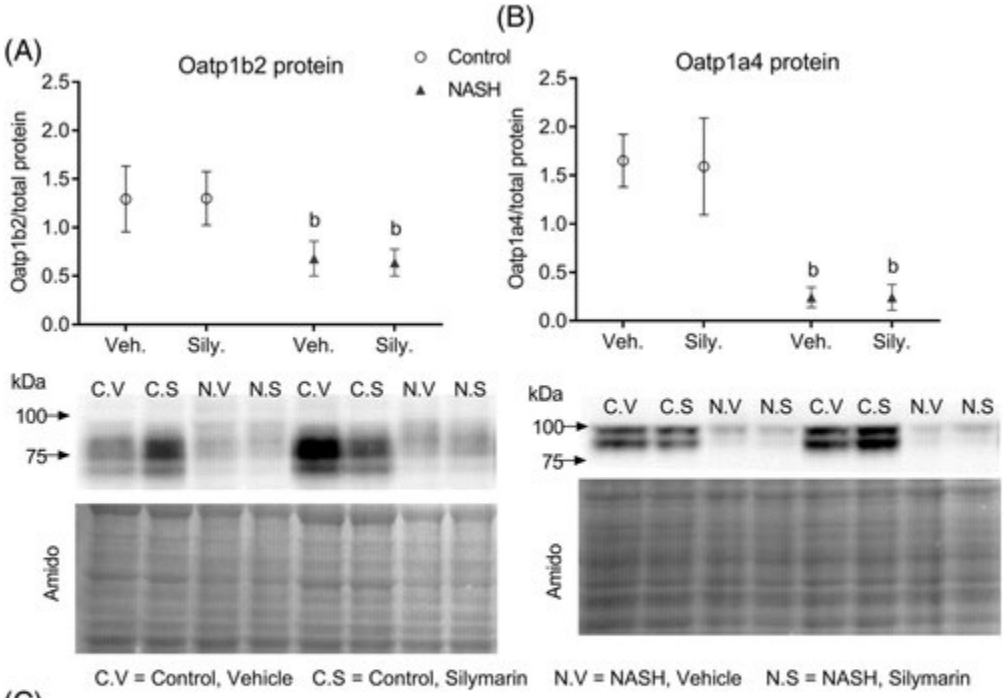


(C)

| 2-way ANOVA | Oatp1b2 protein | Oatp1a4 protein |
|---|---|---|
| NASH | <0.05 | <0.05 |
| Silymarin | 0.95 | 0.84 |
| Interaction | 0.51 | 0.56 |

**FIGURE 3.** Liver Oatp expression. Liver Oatp expression is lower in NASH compared to control animals. Western blot analysis of Oatp1b2 (a) and Oatp1a4 (b) in control and NASH livers 27 hr after pitavastatin oral gavage. Symbols and error bars (a and b) represent means and *SD*s, respectively, of control ($n = 7$) and NASH ($n = 6$) animals. One representative ($n = 2$ for each group) western blot and amido black total protein stain is shown for each protein of interest. Two-way ANOVA p-values are shown in the table (c). Bonferroni post-hoc test $^{b}p$-values $\leq .05$ versus control vehicle group

The contribution of OATPs/Oatps to enteric absorption and hepatic clearance of flavonolignans has not been established. The International Transporter Consortium, composed of the world's experts in drug transporters, highlighted OATP1B1, OATP1B3, and OATP2B1 as clinically important transporters for consideration in drug development, drug-drug interactions, and disease-related changes in drug disposition (Evers et al., 2018; Hillgren et al., 2013; Liang, Li, Zhang, Guo, & Xu, 2011). All tested flavonolignans (SA, SB, IA, IB, SC, and SD) were identified as substrates for OATP1B1, OATP1B3, and OATP2B1 (Figure 2). The amount of SA in the silymarin powdered product used in this study was greater than the amount of SC (>30% vs. <20%) (Montonye et al., 2019), but plasma AUC of SA was 110 times greater than that of SC (Table 1). OATP2B1 is the primary OATP expressed in enterocytes that contributes to the absorption of many drugs and nutrients (Chen, Gibson, Fu, Hu, & Sparreboom, 2019). The apparent lower relative oral bioavailability of SC compared to SA may be partially explained by the lower transport activity of OATP2B1 for SC compared to SA (Figure 2). Species differences in OATP/Oatp isoforms between rodents and humans require analysis of species specific OATP/Oatp isoforms. We confirmed that MCD diet-induced NASH decreased the expression of

Oatp1b2 and Oatp1a4 (Figure 3). Rodent Oatp1b2 is the single ortholog to human OATP1B1 and OATP1B3, and a previous report indicated decreased OATP1B3 expression in NASH patients (Clarke, Novak, Lake, Hardwick, & Cherrington, 2017). Rodent Oatp1a4 is expressed on the sinusoidal membrane of hepatocytes and is involved in the disposition of many xenobiotics, including pitavastatin (Sano et al., 2018). The closest human ortholog to rodent Oatp1a4 is OATP1A2, but OATP1A2 is not expressed in the intestine nor on the sinusoidal membrane of hepatocytes and therefore was not tested (Lee et al., 2005). Decreased OATP/Oatp expression in NASH potentially contributes to higher flavonolignan systemic exposure. Patients with other liver diseases known to decrease OATP expression, such as hepatocellular carcinoma and alcoholic liver disease, may also experience increased flavonolignan systemic exposure, potentially increasing the risk for OATP-mediated silymarin-drug interactions (Obaidat, Roth, & Hagenbuch, 2012; Wang et al., 2016). These data also suggest that the Sprague Dawley MCD NASH model recapitulates the clinical disposition of flavonolignans and taxifolin and can be used to investigate individual and combined effects of silymarin and NASH on the pharmacokinetics of co-consumed drugs.

3.2 Additive pharmacokinetic interaction between silymarin and NASH on pitavastatin exposure

The FDA has made available several guidance documents describing recommendations related to drug development and investigation (FDA, 2020a, 2020b). The current study utilized two guidance documents to produce the most translatable and reliable data needed to evaluate potential hepatic OATP-mediated silymarin-drug interactions (FDA, 2020a, 2020b). First, the guidance for drug interaction studies states that the maximum dose of the precipitant should be used to maximize the possibility of observing a drug-drug interaction. The dose of silymarin in this study was selected to produce plasma flavonolignan concentrations comparable to those observed in humans. Published clinical pharmacokinetic studies in NAFLD and HCV patients showed that 560–700 mg doses of silymarin produced average $C_{max}$ values for SA between 0.8 and 4.2 μM (Fried et al., 2012; Schrieber et al., 2011), and we achieved similar average SA $C_{max}$ values of 1.6 μM for control and 4.5 μM for NASH animals. In addition, pitavastatin was administered first, followed by silymarin, to produce an overlap in $t_{max}$ between pitavastatin and flavonolignans from silymarin (Table 1 and Table 2), maximizing the possibility of a hepatic OATP-mediated interaction. Second, the FDA guidance for in vitro drug interaction studies recommends preincubating cells with the inhibitor when investigating OATP-mediated drug interactions (FDA, 2020a). In the current study, compared to no preincubation, preincubation of OATP-expressing CHO cells with silymarin produced a 2.8-fold leftward shift in $IC_{50}$ for OATP1B1 ($2.8 \pm 0.5$ to $1.0 \pm 0.1$ μg/ml; no preincubation and preincubation, respectively; mean ± *SD*) and a 1.7-fold leftward shift in $IC_{50}$ for both OATP1B3 ($4.5 \pm 1.2$ to $2.6 \pm 0.4$ μg/ml) and OATP2B1 ($1.2 \pm 0.2$ to $0.7 \pm 0.1$ μg/ml) (Figure 4). The FDA recommended R-value (ratio of unbound inhibitor concentration at the liver inlet to $IC_{50}$) cutoff for hepatic OATP-mediated interactions is 1.1. Thus, the lower $IC_{50}$ values with preincubation increase the risk of exceeding 1.1 for potential clinically relevant natural product-drug interactions (FDA, 2020a). These data highlight the importance of recapitulating clinical natural product constituent plasma concentrations and using preincubation for in vitro transporter inhibition experiments when investigating transporter-mediated natural product-drug interactions.

**TABLE 2.** Pitavastatin plasma pharmacokinetics

| | | AUC h*µmol/L | $C_{max}$ µmol/L | $T_{max}$ h |
|---|---|---|---|---|
| Control | Vehicle | 3.1 (2.5, 3.9) | 0.8 (0.5, 1.3) | 0.83 (0.5, 1.0) |
| | Silymarin | 5.7 (5.0, 6.4) | 1.5 (1.2, 1.9) | 1.0 (1.0, 1.0) |
| NASH | Vehicle | 9.1 (6.4, 13.1)[b,c] | 3.1 (1.8, 5.1)[b] | 0.50 (0.25, 0.75)[c] |
| | Silymarin | 15.9 (14.1, 18.1)[a,b,c] | 4.2 (3.1, 5.6)[b,c] | 1.25 (1.0, 2.0)[a,b] |
| Two-way ANOVA | | | | |
| | NASH | <0.05 | <0.05 | 0.62 |
| | Silymarin | <0.05 | 0.03 | <0.05 |
| | Interaction | 0.94 | 0.37 | <0.05 |

*Note:* Data represent geometric means and upper and lower limits of 90% confidence intervals in parentheses for AUC and $C_{max}$. Data for $t_{max}$ represent median with minimum and maximum in parentheses. Oral clearance and terminal half-life could not be recovered due to insufficient data points in the terminal phase of the plasma concentration-time profile. All data shown are based on seven animals for the control group and six animals for the NASH group. Bonferroni post-hoc tests. [a]*p*-values ≤.05 versus respective vehicle groups. [b]*p*-values ≤.05 versus control vehicle group. [c]*p*-values ≤.05 versus control silymarin group.

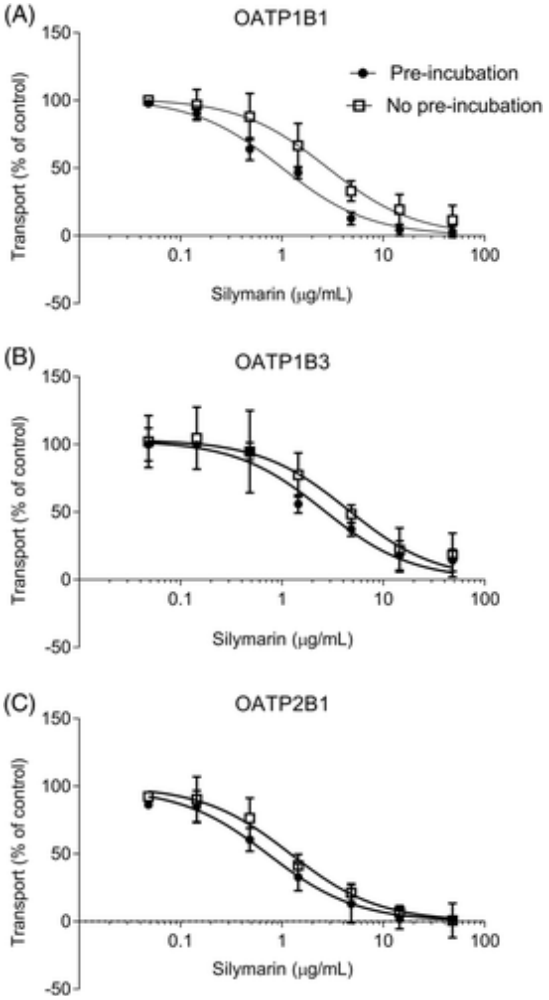


**FIGURE 4.** Silymarin OATP $IC_{50}$ with and without preincubation. The $IC_{50}$ of silymarin against OATPs shifts to the left with preincubation. $IC_{50}$ curves for OATP1B1 (a), OATP1B3 (b), and OATP2B1 (c) using fluorescent probe substrates (dichlorofluorescein, fluorescein, and dibromofluorescein, respectively). Symbols and error bars represent means and *SD*s, respectively, of three replicates. Curves represent model-generated best fit to the data using the standard Hill equation

Pharmacokinetic drug interactions can be precipitated by factors such as genetic polymorphisms, competition of one drug with another drug or a natural product for metabolizing enzymes or transporters, or disease states that alter metabolizing enzyme or transporter expression or function. Multifactorial pharmacokinetic interactions can additively or synergistically affect drug exposure (Clarke et al., 2014; Poller et al., 2019). The current study investigated the effects of orally administered silymarin and diet-induced NASH, both alone and in combination, on oral pitavastatin disposition. Silymarin increased pitavastatin $AUC_{0\text{-}27h}$ 1.8-fold in both the control silymarin and NASH silymarin groups, and NASH alone increased pitavastatin $AUC_{0\text{-}27h}$ 2.9-fold (NASH vehicle compared to control vehicle; Figure 5 and Table 2). The combination of silymarin and NASH increased pitavastatin $AUC_{0\text{-}27h}$ 5.1-fold compared to the control vehicle group (Table 2), demonstrating an additive pharmacokinetic effect of silymarin and NASH on pitavastatin systemic exposure. Pitavastatin is metabolized to pitavastatin lactone by UDP glucuronosyl transferase (UGT) 1A3 and UGT2B7 (Schirris, Ritschel, Bilos, Smeitink, & Russel, 2015), but previous data indicate that inhibition of OATP1B-mediated pitavastatin uptake, rather than UGT-mediated metabolism, increased pitavastatin AUC and did not change pitavastatin lactone AUC (Prueksaritanont et al., 2014). In addition, silybin-mediated inhibition of UGT2B7 only occurs at millimolar concentrations (~0.60–1.5 mM) and was unlikely to contribute to increased pitavastatin AUC in the present study (Uchaipichat, 2018). The 40-min offset between pitavastatin and silymarin administration produced a secondary increase in pitavastatin plasma concentrations from ~40 to 90 min after pitavastatin administration (Figure 5), resulting in no significant silymarin effect on pitavastatin $C_{max}$ (Table 2). Further research is needed to determine whether administration of silymarin simultaneously with pitavastatin produces a single pitavastatin peak and increases pitavastatin $C_{max}$. Compared to control, NASH increased pitavastatin $C_{max}$ by 3.9-fold in the absence of silymarin and 2.8-fold in the presence of silymarin (Table 2). These NASH $C_{max}$ data are consistent with increased plasma concentration of the OATP substrate $^{99m}$Tc-mebrofenin in NASH patients, suggesting that caution may be needed when prescribing narrow therapeutic index drugs dependent on OATPs for systemic clearance to NASH patients (Ali et al., 2018). Liver pitavastatin content was not different between the NASH and control groups; however, the liver to plasma ratio decreased in the NASH group due to higher plasma concentrations at the final time point (Figure 5). The current data did not identify a silymarin effect on pitavastatin liver content in control animals because liver samples were collected after silymarin constituents were largely cleared from the body. The retention of pitavastatin in the plasma in NASH groups at 27 hr suggests that daily administration of pitavastatin in NASH patients may result in higher steady state plasma concentrations and potentially increase the risk of myopathy. These data further support NASH as a determinant of OATP substrate disposition, and that silymarin at 700 mg doses could precipitate OATP-mediated silymarin-drug interactions. In addition, these data provide further evidence that the combination of two precipitants (silymarin and NASH) can cause additive pharmacokinetic effects on the object drug.

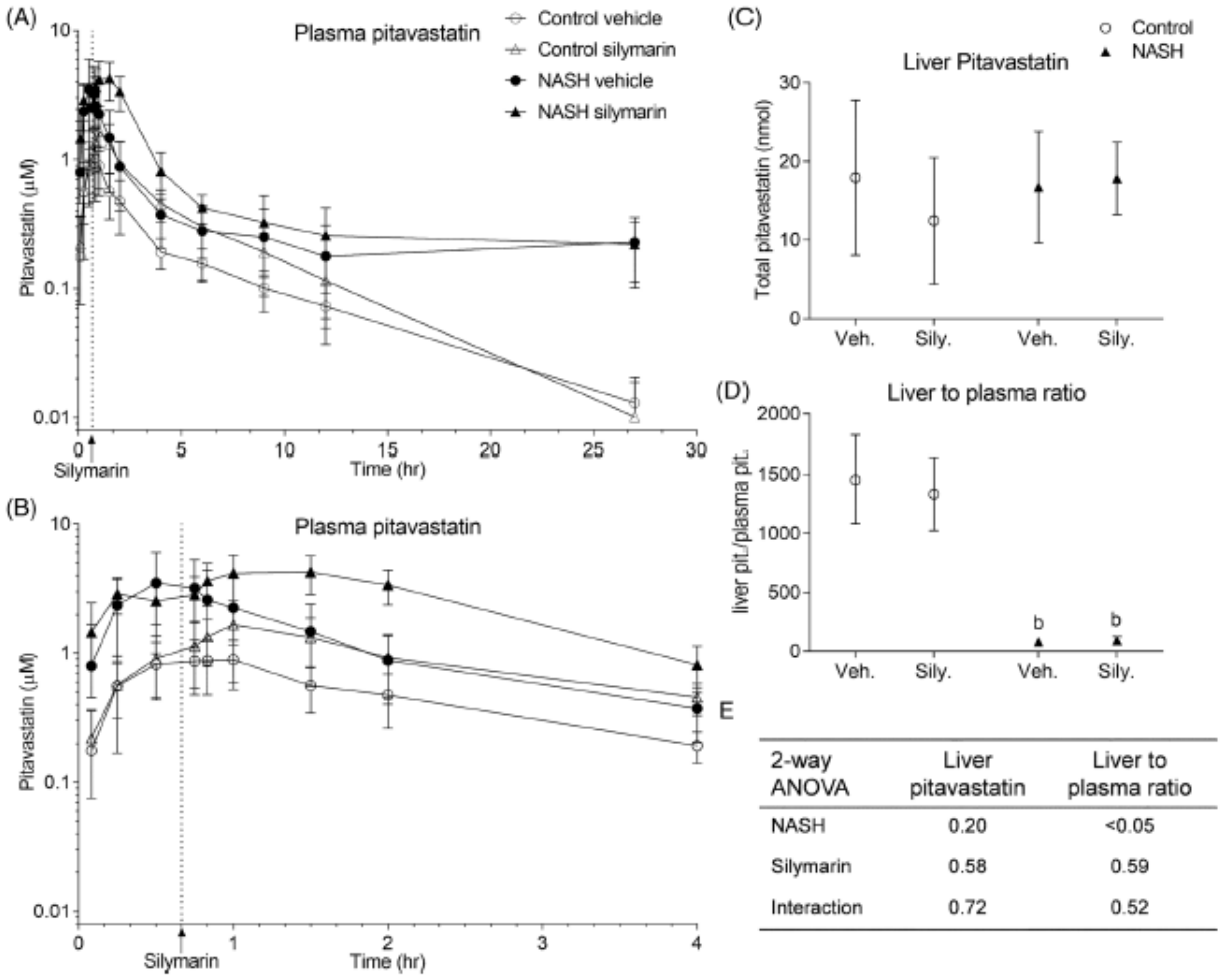


E

| 2-way ANOVA | Liver pitavastatin | Liver to plasma ratio |
|---|---|---|
| NASH | 0.20 | <0.05 |
| Silymarin | 0.58 | 0.59 |
| Interaction | 0.72 | 0.52 |

**FIGURE 5.** Pitavastatin concentration versus time profiles and liver content. Plasma exposure to pitavastatin is higher in NASH compared to control animals in both the absence and presence of silymarin. Average pitavastatin plasma concentration-time profile in control and NASH animals over 27 hr (a) and the first 4 hr (b) after pitavastatin administration by oral gavage (2.5 mg/kg), followed 40 min later by silymarin administration by oral gavage (500 mg/kg). Liver pitavastatin content 27 hr after pitavastatin gavage (c). Ratio of liver pitavastatin content to plasma pitavastatin concentration at 27 hr (d) and corresponding two-way ANOVA *p*-values (e). Bonferroni post-hoc test *p*-values ≤.05 versus control vehicle group. Symbols and error bars represent means and *SD*s, respectively, of control ($n = 7$) and NASH ($n = 6$) animals

## 4 CONCLUSIONS

OATPs/Oatps transport flavonolignans and are important mediators of pharmacokinetic silymarin-drug interactions. Consuming silymarin doses at or above 700 mg may precipitate pharmacokinetic interactions with OATP drug substrates and place patients at risk for adverse drug reactions. In addition, decreased OATP function in liver diseases may be responsible for altered flavonolignan disposition, which may increase flavonolignan systemic exposure and the risk for pharmacokinetic interactions. Specifically, patients with NASH (which decreases OATP expression and function) taking silymarin may be susceptible to an additive pharmacokinetic interaction. Clinical investigation of this silymarin-OATP interaction is warranted to confirm these preclinical observations.

## ACKNOWLEDGMENTS

We kindly thank Dr. Bruno Steiger for providing cell lines. This work was supported in part by the National Institutes of Health, National Center for Complementary and Integrative Health [Grant U54 AT008909] and the Washington State University College of Pharmacy and Pharmaceutical Sciences.

## CONFLICT OF INTEREST

None.

## DATA AVAILABILITY STATEMENT

The data that support the findings of this study are available from the corresponding author upon reasonable request.

## REFERENCES

Abenavoli, L., Izzo, A. A., Milić, N., Cicala, C., Santini, A., & Capasso, R. (2018). Milk thistle (*Silybum marianum*): A concise overview on its chemistry, pharmacological, and nutraceutical uses in liver diseases. *Phytotherapy Research*, **32**(11), 2202– 2213. https://doi.org/10.1002/ptr.6171

Aldridge, G. M., Podrebarac, D. M., Greenough, W. T., & Weiler, I. J. (2008). The use of total protein stains as loading controls: An alternative to high-abundance single-protein controls in semi-quantitative immunoblotting. *Journal of Neuroscience Methods*, **172**(2), 250– 254. https://doi.org/10.1016/j.jneumeth.2008.05.003

Ali, I., Slizgi, J. R., Kaullen, J. D., Ivanovic, M., Niemi, M., Stewart, P. W., … Brouwer, K. L. R. (2018). Transporter-mediated alterations in patients with NASH increase systemic and hepatic exposure to an OATP and MRP2 substrate. *Clinical Pharmacology and Therapeutics*, **104**(4), 749– 756. https://doi.org/10.1002/cpt.997

Bi, X., Yuan, Z., Qu, B., Zhou, H., Liu, Z., & Xie, Y. (2019). Piperine enhances the bioavailability of silybin via inhibition of efflux transporters BCRP and MRP2. *Phytomedicine*, **54**, 98– 108. https://doi.org/10.1016/j.phymed.2018.09.217

Canet, M. J., Hardwick, R. N., Lake, A. D., Dzierlenga, A. L., Clarke, J. D., & Cherrington, N. J. (2014). Modeling human nonalcoholic steatohepatitis-associated changes in drug transporter expression using experimental rodent models. *Drug Metabolism and Disposition*, **42**(4), 586– 595. https://doi.org/10.1124/dmd.113.055996

Chen, M., Gibson, A., Fu, Q., Hu, S., & Sparreboom, A. (2019). Role of OATP2B1 in drug absorption and drug-drug interactions. *The FASEB Journal*, **33**(1), 507.7. https://doi.org/10.1096/FASEBJ.2019.33.1_SUPPLEMENT.507.7

Clarke, J. D., Hardwick, R. N., Lake, A. D., Lickteig, A. J., Goedken, M. J., Klaassen, C. D., & Cherrington, N. J. (2014). Synergistic interaction between genetics and disease on

pravastatin disposition. *Journal of Hepatology*, **61**(1), 139– 147. https://doi.org/10.1016/j.jhep.2014.02.021

Clarke, J. D., Novak, P., Lake, A. D., Hardwick, R. N., & Cherrington, N. J. (2017). Impaired N-linked glycosylation of uptake and efflux transporters in human non-alcoholic fatty liver disease. *Liver International*, **37**(7), 1074– 1081. https://doi.org/10.1111/liv.13362

Deng, J. W., Shon, J.-H., Shin, H.-J., Park, S.-J., Yeo, C.-W., Zhou, H.-H., … Shin, J.-G. (2008). Effect of silymarin supplement on the pharmacokinetics of rosuvastatin. *Pharmaceutical Research*, **25**(8), 1807– 1814. https://doi.org/10.1007/s11095-007-9492-0

Evers, R., Piquette-Miller, M., Polli, J. W., Russel, F. G. M., Sprowl, J. A., Tohyama, K., … International Transporter Consortium. (2018). Disease-associated changes in drug transporters May impact the pharmacokinetics and/or toxicity of drugs: A white paper from the international transporter consortium. *Clinical Pharmacology and Therapeutics*, **104**(5), 900– 915. https://doi.org/10.1002/cpt.1115

FDA. (2020a). In vitro drug interaction studies—Cytochrome P450 enzyme and transporter mediated drug interactions. *Clinical Pharmacology* (pp. 1–46). Retrieved from https://www.fda.gov/regulatory-information/search-fda-guidance-documents/vitro-drug-interaction-studies-cytochrome-p450-enzyme-and-transporter-mediated-drug-interactions

FDA. (2020b). Clinical drug interaction studies-cytochrome P450 enzyme-and transporter-mediated drug interactions guidance for industry. *Clinical Pharmacology*. Retrieved from https://www.fda.gov/regulatory-information/search-fda-guidance-documents/clinical-drug-interaction-studies-cytochrome-p450-enzyme-and-transporter-mediated-drug-interactions

Feher, J., & Lengyel, G. (2012). Silymarin in the prevention and treatment of liver diseases and primary liver cancer. *Current Pharmaceutical Biotechnology*, **13**(1), 210– 217. https://doi.org/10.2174/138920112798868818

Flaig, T. W., Gustafson, D. L., Su, L.-J. J., Zirrolli, J. A., Crighton, F., Harrison, G. S., … Glodé, L. M. (2007). A phase I and pharmacokinetic study of silybin-phytosome in prostate cancer patients. *Investigational New Drugs*, **25**(2), 139– 146. https://doi.org/10.1007/s10637-006-9019-2

Fried, M. W. (2012). Effect of Silymarin (Milk thistle) on liver disease in patients with chronic hepatitis C unsuccessfully treated with interferon therapy. *JAMA*, **308**(3), 274– 282. https://doi.org/10.1001/jama.2012.8265

Fried, M. W., Navarro, V. J., Afdhal, N., Belle, S. H., Wahed, A. S., Hawke, R. L., … Reddy, K. R. (2012). Effect of silymarin (milk thistle) on liver disease in patients with chronic hepatitis C unsuccessfully treated with interferon therapy: A randomized controlled trial. *JAMA—Journal of the American Medical Association*, **308**(3), 274– 282. https://doi.org/10.1001/jama.2012.8265

Gao, X., Xiao, Z. H., Liu, M., Zhang, N. Y., Khalil, M. M., Gu, C. Q., … Sun, L. H. (2018). Dietary silymarin supplementation alleviates zearalenone-induced

hepatotoxicity and reproductive toxicity in rats. *Journal of Nutrition*, **148**(8), 1209– 1216. https://doi.org/10.1093/jn/nxy114

Giacomini, K. M., Huang, S. M., Tweedie, D. J., Benet, L. Z., Brouwer, K. L., Chu, X., … Zhang, L. (2010). Membrane transporters in drug development. *Nature Reviews Drug Discovery*, **9**(3), 215– 236. https://doi.org/10.1038/nrd3028

Graf, T. N., Cech, N. B., Polyak, S. J., & Oberlies, N. H. (2016). A validated UHPLC-tandem mass spectrometry method for quantitative analysis of flavonolignans in milk thistle (*Silybum marianum*) extracts. *Journal of Pharmaceutical and Biomedical Analysis*, **126**, 26– 33. https://doi.org/10.1016/j.jpba.2016.04.028

Graf, T., Wani, M., Agarwal, R., Kroll, D., & Oberlies, N. (2007). Gram-scale purification of flavonolignan diastereoisomers from *Silybum marianum* (Milk thistle) extract in support of preclinical *in vivo* studies for prostate cancer chemoprevention. *Planta Medica*, **73**(14), 1495– 1501. https://doi.org/10.1055/s-2007-990239

Gufford, B. T., Chen, G., Lazarus, P., Graf, T. N., Oberlies, N. H., & Paine, M. F. (2014). Identification of diet-derived constituents as potent inhibitors of intestinal glucuronidation. *Drug Metabolism and Disposition*, **42**(10), 1675– 1683. https://doi.org/10.1124/dmd.114.059451

Gufford, B. T., Graf, T. N., Paguigan, N. D., Oberlies, N. H., & Paine, M. F. (2015). Chemoenzymatic synthesis, characterization, and scale-up of milk thistle flavonolignan glucuronides. *Drug Metabolism and Disposition*, **43**(11), 1734– 1743. https://doi.org/10.1124/dmd.115.066076

Hagenbuch, B., & Meier, P. J. (2004). Organic anion transporting polypeptides of the OATP/SLC21 family: Phylogenetic classification as OATP/SLCO superfamily, new nomenclature and molecular/functional properties. *Pflügers Archiv: European Journal of Physiology*, **447**, 653– 665. https://doi.org/10.1007/s00424-003-1168-y

Heinrich, M., Appendino, G., Efferth, T., Fürst, R., Izzo, A. A., Kayser, O., … Viljoen, A. (2020). Best practice in research—Overcoming common challenges in phytopharmacological research. *Journal of Ethnopharmacology*, **246**, 112230. https://doi.org/10.1016/j.jep.2019.112230

Hillgren, K. M., Keppler, D., Zur, A. A., Giacomini, K. M., Stieger, B., Cass, C. E., … International Transporter Consortium. (2013). Emerging transporters of clinical importance: An update from the international transporter consortium. *Clinical Pharmacology and Therapeutics*, **94**(1), 52– 63. https://doi.org/10.1038/clpt.2013.74

Izumi, S., Nozaki, Y., Komori, T., Takenaka, O., Maeda, K., Kusuhara, H., & Sugiyama, Y. (2016). Investigation of fluorescein derivatives as substrates of organic anion transporting polypeptide (OATP) 1B1 to develop sensitive fluorescence-based OATP1B1 inhibition assays. *Molecular Pharmaceutics*, **13**(2), 438– 448. https://doi.org/10.1021/acs.molpharmaceut.5b00664

Izzo, A. A., Teixeira, M., Alexander, S. P. H., Cirino, G., Docherty, J. R., George, C. H., … Ahluwalia, A. (2020). A practical guide for transparent reporting of research on natural products in the *British Journal of Pharmacology*: Reproducibility of natural

product research. *British Journal of Pharmacology*, **177**(10), 2169– 2178. https://doi.org/10.1111/bph.15054

Javed, S., Kohli, K., & Ali, M. (2011). Reassessing bioavailability of silymarin. *Alternative Medicine Review*, **16**(3), 239– 249.

Kellogg, J. J., Paine, M. F., McCune, J. S., Oberlies, N. H., & Cech, N. B. (2019). Selection and characterization of botanical natural products for research studies: A NaPDI center recommended approach. *Natural Product Reports*, **36**(8), 1196– 1221. https://doi.org/10.1039/c8np00065d

Lee, W., Glaeser, H., Smith, L. H., Roberts, R. L., Moeckel, G. W., Gervasini, G., … Kim, R. B. (2005). Polymorphisms in human organic anion-transporting polypeptide 1A2 (OATP1A2): Implications for altered drug disposition and central nervous system drug entry. *Journal of Biological Chemistry*, **280**(10), 9610– 9617. https://doi.org/10.1074/jbc.M411092200

Liang, J., Li, T., Zhang, Y.-L., Guo, Z.-L., & Xu, L.-H. (2011). Effect of microcystin-LR on protein phosphatase 2A and its function in human amniotic epithelial cells. *Journal of Zhejiang University Science B*, **12**(12), 951– 960. https://doi.org/10.1631/jzus.B1100121

Lieber, C. S., Leo, M. A., Cao, Q., Ren, C., & DeCarli, L. M. (2003). Silymarin retards the progression of alcohol-induced hepatic fibrosis in baboons. *Journal of Clinical Gastroenterology*, **37**(4), 336– 339. https://doi.org/10.1097/00004836-200310000-00013

Maeda, K. (2015). Organic anion transporting polypeptide (OATP)1B1 and OATP1B3 as important regulators of the pharmacokinetics of substrate drugs. *Biological & Pharmaceutical Bulletin*, **38**(2), 155– 168. https://doi.org/10.1248/bpb.b14-00767

Miranda, S. R., Jin, K. L., Brouwer, K. L. R., Wen, Z., Smith, P. C., & Hawke, R. L. (2008). Hepatic metabolism and biliary excretion of silymarin flavonolignans in isolated perfused rat livers: Role of multidrug resistance-associated protein 2 (Abcc2). *Drug Metabolism and Disposition*, **36**(11), 2219– 2226. https://doi.org/10.1124/dmd.108.021790

Montonye, M. L., Tian, D.-D., Arman, T., Lynch, K. D., Hagenbuch, B., Paine, M. F., & Clarke, J. D. (2019). A pharmacokinetic natural product-disease-drug interaction: A double hit of Silymarin and nonalcoholic steatohepatitis on hepatic transporters in a rat model. *Journal of Pharmacology and Experimental Therapeutics*, **371**(2), 385– 393. https://doi.org/10.1124/jpet.119.260489

Müzes, G., Deák, G., Láng, I., Nékám, K., Niederland, V., & Fehér, J. (1990). Effect of silimarin (Legalon) therapy on the antioxidant defense mechanism and lipid peroxidation in alcoholic liver disease (double blind protocol). *Orvosi Hetilap*, **131**(16), 863– 866.

Obaidat, A., Roth, M., & Hagenbuch, B. (2012). The expression and function of organic anion transporting polypeptides in normal tissues and in cancer. *Annual Review of Pharmacology and Toxicology*, **52**, 135– 151. https://doi.org/10.1146/annurev-pharmtox-010510-100556

Poller, B., Woessner, R., Barve, A., Tillmann, H.-C., Vemula, J., Nica, A., … Weiss, M. (2019). Fevipiprant has a low risk of influencing co-medication pharmacokinetics: Impact on simvastatin and rosuvastatin in different SLCO1B1 genotypes. *Pulmonary Pharmacology & Therapeutics*, **57**, 101809. https://doi.org/10.1016/j.pupt.2019.101809

Prueksaritanont, T., Chu, X., Evers, R., Klopfer, S. O., Caro, L., Kothare, P. A., … Stoch, S. A. (2014). Pitavastatin is a more sensitive and selective organic anion-transporting polypeptide 1B clinical probe than rosuvastatin. *British Journal of Clinical Pharmacology*, **78**(3), 587– 598. https://doi.org/10.1111/bcp.12377

Qi, X., Ding, L., Wen, A., Zhou, N., Du, X., & Shakya, S. (2013). Simple LC-MS/MS methods for simultaneous determination of pitavastatin and its lactone metabolite in human plasma and urine involving a procedure for inhibiting the conversion of pitavastatin lactone to pitavastatin in plasma and its application to a phar. *Journal of Pharmaceutical and Biomedical Analysis*, **72**, 8– 15. https://doi.org/10.1016/j.jpba.2012.09.026

Sano, Y., Mizuno, T., Mochizuki, T., Uchida, Y., Umetsu, M., Terasaki, T., & Kusuhara, H. (2018). Evaluation of organic anion transporter 1A2-knock-in mice as a model of human blood-brain barrier. *Drug Metabolism and Disposition*, **46**(11), 1767– 1775. https://doi.org/10.1124/dmd.118.081877

Schirris, T. J. J., Ritschel, T., Bilos, A., Smeitink, J. A. M., & Russel, F. G. M. (2015). Statin Lactonization by Uridine 5′-Diphospho-glucuronosyltransferases (UGTs). *Molecular Pharmaceutics*, **12**(11), 4048– 4055. https://doi.org/10.1021/acs.molpharmaceut.5b00474

Schrieber, S. J., Hawke, R. L., Wen, Z., Smith, P. C., Reddy, K. R., Wahed, A. S., … Fried, M. W. (2011). Differences in the disposition of silymarin between patients with nonalcoholic fatty liver disease and chronic hepatitis C. *Drug Metabolism and Disposition*, **39**(12), 2182– 2190. https://doi.org/10.1124/dmd.111.040212

Schrieber, S. J., Wen, Z., Vourvahis, M., Smith, P. C., Fried, M. W., Kashuba, A. D. M., & Hawke, R. L. (2008). The pharmacokinetics of silymarin is altered in patients with hepatitis C virus and nonalcoholic fatty liver disease and correlates with plasma caspase-3/7 activity. *Drug Metabolism and Disposition*, **36**(9), 1909– 1916. https://doi.org/10.1124/dmd.107.019604

Smith, T., May, G., Eckl, V., & Reynolds, C. M. (2020). US Sales of Herbal Supplements Increase by 8.6% in 2019. *Herbalgram*. Retrieved from www.herbalgram.org

Uchaipichat, V. (2018). In vitro inhibitory effects of major bioactive constituents of *Andrographis paniculata*, Curcuma longa and *Silybum marianum* on human liver microsomal morphine glucuronidation: A prediction of potential herb-drug interactions arising from andrographolide, curcumin and silybin inhibition in humans. *Drug Metabolism and Pharmacokinetics*, **33**(1), 67– 76. https://doi.org/10.1016/j.dmpk.2017.10.005

Voroneanu, L., Nistor, I., Dumea, R., Apetrii, M., & Covic, A. (2016). Silymarin in type 2 diabetes mellitus: A systematic review and meta-analysis of randomized controlled trials. *Journal of Diabetes Research*, **2016**, 1– 10. https://doi.org/10.1155/2016/5147468

Wah Kheong, C., Nik Mustapha, N. R., & Mahadeva, S. (2017). A randomized trial of Silymarin for the treatment of nonalcoholic Steatohepatitis. *Clinical Gastroenterology and Hepatology*, **15**(12), 1940– 1949. https://doi.org/10.1016/j.cgh.2017.04.016

Wang, L., Collins, C., Kelly, E. J., Chu, X., Ray, A. S., Salphati, L., … Unadkat, J. D. (2016). Transporter expression in liver tissue from subjects with alcoholic or hepatitis C cirrhosis quantified by targeted quantitative proteomics. *Drug Metabolism and Disposition*, **44**(11), 1752– 1758. https://doi.org/10.1124/dmd.116.071050

Wen, Z., Dumas, T. E., Schrieber, S. J., Hawke, R. L., Fried, M. W., & Smith, P. C. (2008). Pharmacokinetics and metabolic profile of free, conjugated, and total silymarin flavonolignans in human plasma after oral administration of milk thistle extract. *Drug Metabolism and Disposition: The Biological Fate of Chemicals*, **36**(1), 65– 72. https://doi.org/10.1124/dmd.107.017566

Wlcek, K., Koller, F., Ferenci, P., & Stieger, B. (2013). Hepatocellular organic anion-transporting polypeptides (OATPs) and multidrug resistance-associated protein 2 (MRP2) are inhibited by silibinin. *Drug Metabolism and Disposition*, **41**(8), 1522– 1528. https://doi.org/10.1124/dmd.113.051037

Xu, P., Zhou, H., Li, Y. Z., Yuan, Z. W., Liu, C. X., Liu, L., & Xie, Y. (2018). Baicalein enhances the oral bioavailability and hepatoprotective effects of silybin through the inhibition of efflux transporters BCRP and MRP2. *Frontiers in Pharmacology*, **9**, 1115. https://doi.org/10.3389/fphar.2018.01115